RADIATION RESEARCH 133, 41–51 (1993)

The Response of Chinese Hamster V79 Cells to Low Radiation Doses: Evidence of Enhanced Sensitivity of the Whole Cell Population

B. MARPLES AND M. C. JOINER

CRC Gray Laboratory, P.O. Box 100, Mount Vernon Hospital, Northwood, Middlesex HA6 2JR, United Kingdom

MARPLES, B., AND JOINER, M. C. The Response of Chinese Hamster V79 Cells to Low Radiation Doses: Evidence of Enhanced Sensitivity of the Whole Cell Population. *Radiat. Res.* 133, 41–51 (1993).

High-resolution measurements of the survival of asynchronous Chinese hamster V79–379A cells *in vitro* after single doses of X rays (0.01–10.0 Gy) and neutrons (0.02–3.0 Gy) were made using a computerized microscope for locating and identifying cells (Palcic and Jaggi, *Int. J. Radiat. Biol.* 50, 345–352, 1986). The X-ray response from 1 to 10 Gy showed a good fit to a linear-quadratic (LQ) dose–survival model, but with X-ray doses below 0.6 Gy, an *increased* X-ray effectiveness was observed, with cell survival below the prediction made from the data above 1 Gy using the LQ model. The effect per unit dose ($-\log_e$SF/dose) increased by a factor of ~2, from 0.19 Gy^{-1} at a dose of 1 Gy to 0.37 Gy^{-1} at a dose of 0.1 Gy. This phenomenon was not seen with neutrons, and cell survival decreased exponentially over the whole neutron dose range studied. Further data suggest that this phenomenon is unlikely to be due to a subpopulation of X-ray-sensitive cells determined either genetically or phenotypically by distribution of the population within the cell cycle. The existence of low-dose sensitivity also appeared to be independent of dose rate in the range 0.016–1.7 Gy min^{-1}. A possible explanation of these results is that the phenomenon reflects "induced repair" or a stress response: low doses *in vitro* (or low doses per fraction *in vivo*) are more effective per gray than higher doses because only at the higher doses is there sufficient damage to trigger repair systems or other radioprotective mechanisms.

INTRODUCTION

After moderate to large radiation doses (2–20 Gy), mammalian cell survival is measured conventionally with the clonogenic assay devised by Puck and Marcus (*1*). Typically, however, this assay is not sufficiently precise to measure the very small reduction in cell survival which results from irradiating with doses less than ~1 Gy, owing to uncertainty in the number of cells plated in each culture dish due to random errors in cell counting, dilution, and plating procedures (*2, 3*). Therefore, the shape of the mammalian cell survival curve at low doses has often been derived by extrapolation, from mathematical fits of radiobiological models to experimental data obtained at higher doses (e.g., 4). It has been demonstrated that the low-dose response obtained in this way is dependent upon the model used to describe the high-dose data (*5, 6*), and therefore the validity of such extrapolations has been questioned (*7–9*).

To overcome the poor resolution of the Puck and Marcus assay at low doses, several experimental techniques which determine the number of cells assayed with a greater precision have been used (*3, 6, 10–15*). They can be classified broadly into two categories: those methods which measure cell survival by conventional colony formation from a more precisely known number of cells plated (*3, 6, 13, 14*) and those methods which select a *specific* set of cells from a sample *after* plating and follow each of these cells individually to determine whether each forms a colony or not (*10, 11, 15*). Such methods have been employed to measure oxygen and sensitizer enhancement ratios after exposure to low radiation doses and have demonstrated that the OER (*8, 9*) and some SERs (*6, 11*) are lower than values predicted by extrapolation from higher-dose data. These studies exemplify the importance of directly measuring low-dose cell survival and the unreliability of extrapolating from high doses as a substitute.

In the study described in this paper, the radiation response of mammalian cells to very low doses of X rays and neutrons was determined and compared, using a dynamic microscopic image processing scanner (DMIPS) cell analyzer (*12*) capable of locating and identifying freshly plated cells and following these individually to determine colony formation.

MATERIALS AND METHODS

Cells. Chinese hamster V79–379A cells were maintained routinely in suspension culture in Eagle's minimal essential medium with reduced calcium (MEM-S), supplemented with 7.5% (v/v) fetal calf serum (FCS). Cells were kept in exponential growth by daily dilution with fresh culture medium supplemented with serum. Although this V79 subline has been adapted specifically to grow in suspension culture, it retains the ability to grow as a monolayer in Eagle's calcium-containing α-MEM supplemented with 10% FCS.

Irradiations. Cells were irradiated with X rays at room temperature (21–24°C) in sealed culture flasks or in equilibrium with air as suspension cultures (*6*). The cells were maintained in an incubator at 37°C in humidi-

0033-7587/93 $5.00

fied air plus 5% CO_2 immediately prior to and following radiation treatment. Irradiation was with 250-kVp X rays (HVL = 1.46 mm Cu) at dose rates of 0.016 Gy min^{-1} (0.01–0.5 Gy), 0.44 Gy min^{-1} (0.2–5 Gy), or 1.7 Gy min^{-1} (1–10 Gy). The dose rate was varied by changing the distance between the X-ray head and the culture flask and was selected according to the dose delivered so that exposure times were always greater than 25 s to maintain dosimetric accuracy, the shutter on the X-ray set taking $\leq$1.5 s to open. In some experiments, 2.5-MVp X rays were produced by focusing electrons from a Van de Graaff accelerator onto a gold target and a range of dose rates from 0.004 to 6 Gy min^{-1} was achieved by varying the electron beam current from 7 to 200 μA.

Cells were irradiated with neutrons using the same handling procedures. d(4)-Be neutrons (60–70 keV μm^{-1}) were produced using the Van de Graaff accelerator by bombarding a thick beryllium target with 4-MeV deuterons. The neutron dose rate was 0.2 Gy min^{-1}.

Conventional colony assay. Cells in exponential growth were irradiated in suspension at room temperature in 25 ml MEM-S + 7.5% FCS containing 4×10^5 cells ml^{-1}. During irradiation, the cell suspension was stirred continuously using a magnetic stirrer. Cell samples were removed sequentially at specified doses and diluted serially with α-MEM supplemented with 10% FCS, and aliquots were pipetted into tissue culture-grade plastic dishes. Dishes were incubated at 37°C in a water-saturated atmosphere of 95% air + 5% CO_2 for 7 days and then stained, and colonies containing $\geq$50 cells were scored as representing surviving cells from the original irradiated suspension.

DMIPS recognition assay. A sample from a stock suspension culture in exponential growth was serially diluted and approximately 3000 cells were plated into 25-cm^2 tissue culture flasks (Nunclon 152074) in 5 ml of α-MEM. Ninety minutes of incubation at 37°C in a water-saturated atmosphere of 95% air + 5% CO_2 was allowed for the cells to attach to the bottom surface of the flask. The culture medium was then removed by pouring it off slowly over the upper (non-cell) side of the flask, which was immediately refilled completely (to 40 ml), over the same surface, with fresh medium prewarmed to 37°C and equilibrated with 5% CO_2, and sealed. Following irradiation, the DMIPS cell analyzer was used to locate and record the positions of cells in a 10-cm^2 area in the center of the tissue culture flask. During this scan, the temperature around the flask was kept at 37°C with a thermostatically controlled microscope incubator. Following scanning, sealed flasks were incubated at 37°C for 3.5 days, sufficient to allow six or seven divisions in this cell line to produce colonies of greater than 50 cells from a single surviving cell. At this time, flasks were rescanned and the location of each recorded cell was revisited automatically to detect if a colony was present and, if so, to measure its size. The fraction of surviving cells at each dose level in both assays was determined as the plating efficiency (irradiated cells)/plating efficiency (unirradiated cells).

In some experiments using the DMIPS assay, cells were irradiated in suspension using a protocol identical to that of the conventional assay. Cell samples, removed sequentially at specified doses, were diluted and aliquots plated for 90 min in 5 ml of α-MEM to allow time for attachment to the surface of the culture flask. The medium was then removed, and the flask was refilled and scanned to locate and record the positions of cells as described above.

Cell recognition algorithms. The theory and operation of the DMIPS cell analyzer and its software have been described in detail (*12, 15, 16*). Briefly, the cell detection software incorporates an algorithm specific for each cell line for recognizing objects and then discriminating freshly plated single live cells from all other objects (e.g., debris, scratches on the culture surface, dead cells, and doublets) that might be present in the culture flask. Freshly plated cells initially attach onto the growth surface in a spherical "rounded-up" shape and gradually flatten out over a 4- to 5-h period. While the cell is rounded up, when optimally focused (*17*), it behaves as a small lens focusing parallel light toward its center and producing a characteristic image with a bright center surrounded by a dark rim. The DMIPS machine extracts and records 18 individual features from a single line of this image and compares these measurements with a master set of distributions of values of the 18 features determined previously from a large population of known viable cells typical of the cell line under investigation. The algorithm first excludes any object from the sample if the value of any feature from the object signal falls outside typical upper and lower limits determined by the master parameter file. It then applies a discriminant function to the remaining data to distinguish further the cells from other objects. Under normal culture procedures, the false-positive error, i.e., debris being classified as cells, was $\leq$4%. This was reduced further by routinely passing the culture medium through a 0.22-μm Millipore filter immediately before use; this removed much of the debris due to serum protein precipitation and reduced further the possibility that a piece of debris would be incorrectly recognized as a cell. With these precautions, the false-positive error in recognition was routinely $\leq$2% while the false-negative error was $\leq$9%.

Construction of cell recognition algorithms for cells in specific phases of the cell cycle. The master V79-379A parameter file used for the majority of the experiments was constructed from images of cells in asynchronous populations. However, populations of *synchronized* cells obtained by centrifugal elutriation (Beckman J6B elutriator) were also used to construct parameter files which enabled the DMIPS cell analyzer to locate and detect cells in G_1 and S phase automatically from within a freshly plated asynchronous population. The distinction between cells in different stages of the cycle is largely dependent on size, but using all 18 features of the cell image results in an identification of cell cycle phase with a good degree of accuracy. Using these specific recognition algorithms, the DMIPS was used to measure the response of G_1- or S-phase cells to low radiation doses. These algorithms proved as efficient at selecting G_1- or S-phase cells as elutriation (Table I); additionally, the DMIPS method was quicker and more dependable than using an elutriator and did not result in the cells being exposed to physical stress during any synchronization procedure.

TABLE I

Fraction (%) of Eluted Populations of Cells Recognized in Different Phases of the Cell Cycle by Flow Cytometry (FCM) (*38*), or DMIPS Using Phase-Specific Recognition Algorithms

	FCM shows cells in		
	G_1 phase	S phase	G_2 + M phase
G_1-phase enriched	90 ± 2	9 ± 2	1 ± 1
S-phase enriched	17 ± 6	71 ± 9	12 ± 14
Asynchronous	51 ± 4	43 ± 5	6 ± 2

	DMIPS shows cells in			
	G_1 phase	True +ve	S phase	True +ve
G_1-phase enriched	80 ± 8	87 ± 8	14 ± 2	—
S-phase enriched	12 ± 3	—	71 ± 6	84 ± 7
Asynchronous	49 ± 9	84 ± 6	38 ± 7	83 ± 5

Note. Values designated "True +ve" are the percentage of those cells recognized in the G_1 and S phases which were confirmed by measuring time to mitosis or immediate labeling with bromodeoxyuridine, respectively. Values are the mean of at least three assessments on different cell populations, ±SD.

RESULTS

A comparison between cell survival measured using the DMIPS assay and the conventional assay is shown in Fig. 1.

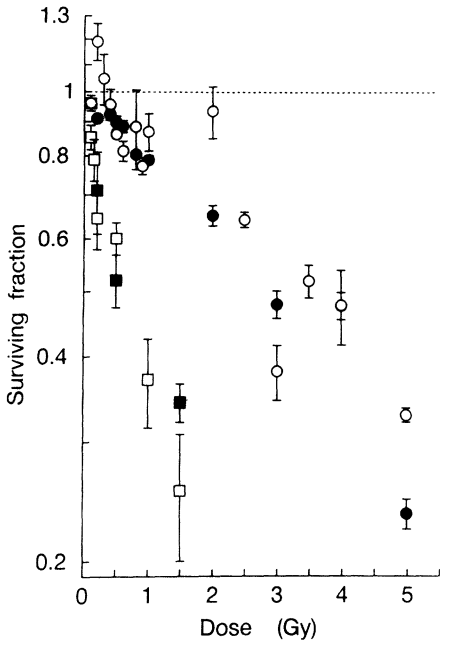

FIG. 1. Survival of cells irradiated with 250-kVp X rays (●, ○) and d(4)-Be neutrons (○, □) obtained using a conventional clonogenic assay (open symbols) and the DMIPS assay (closed symbols). Each point represents the mean survival from at least three replicate dishes or flasks ± SEM. The variability in the measurements made by the conventional assay is typical at such high survival levels and is considerably reduced by using the DMIPS assay.

Both assays gave similar values of surviving fraction over the high-dose range (1–4 Gy); however, the variation in the conventional measurements is larger, especially at X-ray doses below 1 Gy, as expected. This is partly a consequence of the uncertainty in the precise number of cells plated in the conventional assay (*2*), which is not a problem with the DMIPS procedure because the number of cells assayed is determined *after* plating when the cells have attached to the growth surface.

Typical survival curves for X rays (0.01–5 Gy) and neutrons (0.02–1.5 Gy) obtained with the DMIPS assay are shown in Fig. 2. The neutron data were always well fitted with a single exponential function; no consistent deviation from linearity on these semilogarithmic plots was seen. The X-ray response was found to be multiphasic; survival estimates over the dose range 1–10 Gy showed a good fit to an LQ model, whereas for doses < 0.5 Gy a significantly increased X-ray sensitivity was observed with survival determinations below the extrapolation obtained from the fit of the LQ model at doses ≥ 1 Gy.

These data suggest that X-ray doses in the range 0–0.3 Gy may be more effective "per unit dose" at killing cells than doses > 1 Gy. Figure 3 shows the data from all the experiments in the study, plotted as $-\text{dose}/\log_e(\text{SF})$; this is the inverse slope of the chord joining the zero-dose origin of the survival curve (plotted on log-linear axes) to a given point on the survival curve expressed as an "effective D_0." Figure 3a suggests that over the dose range 0.02–3 Gy, neutrons are equally effective per unit dose at killing cells and so effective D_0 is (on average) constant, reflecting a single-exponential survival curve. In contrast, X rays (Fig. 3b) become less effective as the dose increases from zero, being minimally effective (with maximum effective D_0) at about 0.6–1 Gy and then becoming more effective again as the dose increases above 1.5 Gy. This pattern reflects the complex low-dose shape of the X-ray survival curve shown in Fig. 2.

Small differences in cellular radiosensitivity between individual experiments were identified as one possible source of variance in low-dose studies (*2*). In the present study, both X-ray and neutron survival were measured together in each of the experiments contributing to the data shown in Fig. 3. Since neutron survival was found to be exponential (Figs. 2 and 3a) it could be used simply as an internal reference for the X-ray response measured in each experiment, the rationale being that interexperimental differences in radiosensitivity might be in similar proportion for X rays and neutrons and so would be reduced in a comparison of relative doses needed to produce the same effect, i.e., the relative biological effectiveness (RBE). Within each experiment, an RBE was calculated for each X-ray data point by

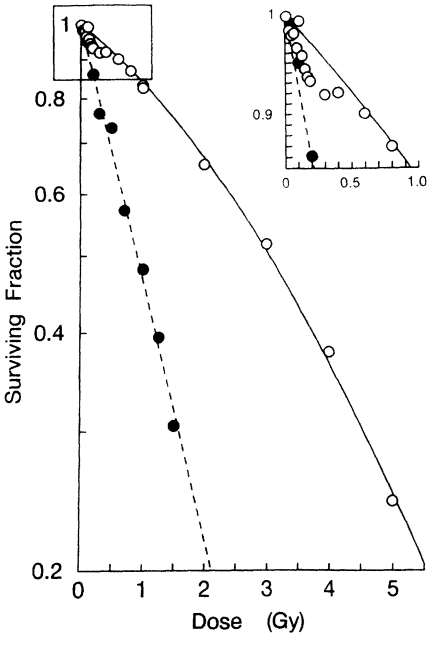

FIG. 2. Survival of cells measured with the DMIPS assay in a typical experiment. Cells were irradiated attached to plastic with 250-kVp X rays (○) or d(4)-Be neutrons (●). Each point represents a single measurement of surviving fraction on 300–400 cells. The solid line shows the fit of the linear-quadratic model to the X-ray data above 1 Gy. The straight dashed line shows the fit of a single exponential function to all the neutron data. The inset shows the low-dose region of the survival curves expanded and demonstrates the increased effectiveness of X rays below 0.5 Gy compared to the LQ prediction.

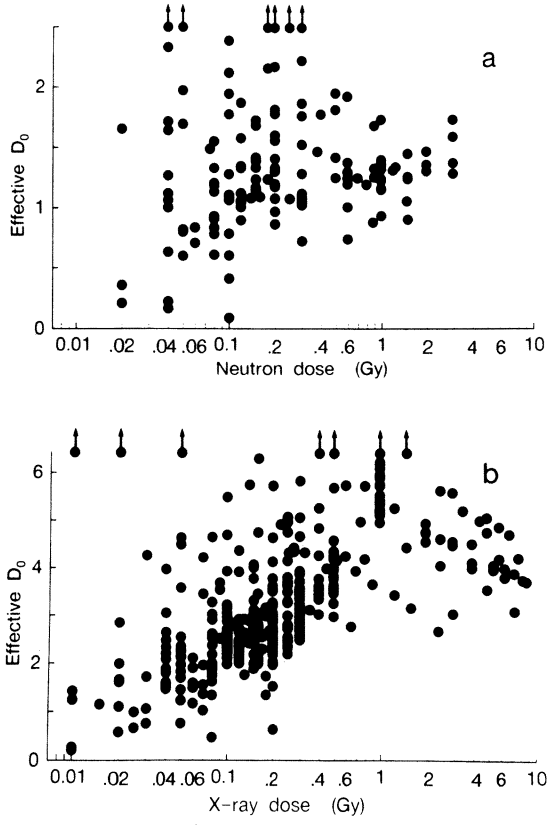

FIG. 3. Effective D_0 (see text) plotted against radiation dose, for each individual measurement of survival after irradiation by either d(4)-Be neutrons (a) or 250-kVp X rays (b). Upward arrows indicate data values beyond the *y* axis shown. In this complete data set there are 146 measurements of surviving fraction after neutrons and 364 measurements of surviving fraction after X rays. There is no trend in the neutron data but the X-ray data show an increased effectiveness of radiation as the dose is decreased below 1 Gy.

dividing the X-ray dose given by the neutron dose required for isosurvival, obtained by back substitution into the exponential equation obtained by fitting a straight line to the values of $\log_e$ (surviving fraction) versus neutron dose by linear regression. Figure 4 summarizes the complete data set of 364 X-ray survival measurements in 56 experiments, expressed as RBEs. The increase in X-ray radioresistance from 0.01–0.6 Gy seen in Figs. 2 and 3b is paralleled by an increase in RBE over the same dose range. At very low doses, the RBE is significantly lower; hence X rays are significantly more effective per unit dose, compared with a prediction from a linear-quadratic model based on data at doses $\geq$ 1 Gy (shown dashed). The same pattern of increasing RBE with increasing X-ray dose over the range 0.01–1 Gy, demonstrated in Fig. 4, was also seen when cells were irradiated in suspension culture (data not shown), indicating that the increasing X-ray radioresistance seen over this dose range was not a consequence of irradiating cells as attached monolayers.

If the multicomponent X-ray survival curves (reflected by the increase in RBE with increasing X-ray dose) were due to the existence of two subpopulations of cells of different radiosensitivities, then these subpopulations might be determined either genetically or phenotypically by, for example, distribution within the cell cycle. The data in Fig. 5 show that a cell population irradiated 24 h previously with 1 Gy exhibited the same type of response to subsequent irradiation as previously unirradiated cells. The data in Fig. 6 show that cells cloned from a single cell of the parental stock cell culture also demonstrated the same survival response, with increased low-dose sensitivity. These two experiments indicate that the shape of the X-ray survival response seen in Figs. 2, 3, and 4 is unlikely to be due to a genetically determined sensitive subpopulation of cells in the pre-irradiated cultures.

It has been suggested that regions of inflexion or sub-

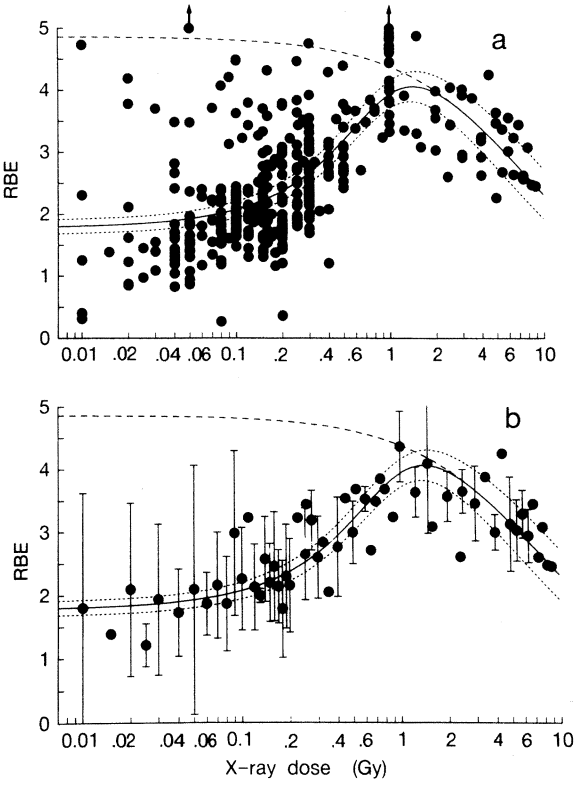

FIG. 4. Relative biological effectiveness (RBE) between 250-kVp X rays and d(4)-Be neutrons plotted against X-ray dose. Smaller RBE means greater X-ray effect per unit dose. The RBE value was calculated for each individual measurement of X-ray survival, relative to the fit to the neutron data obtained within the same experiment (see text). Panel (a) shows all the individual measurements and panel (b) shows the data as mean values ± SD. Solid lines show the fit of an "induced repair" model to the data (see text) with 95% confidence limits on the mean (expected) prediction shown as dotted lines. The dashed lines show how a linear-quadratic model of X-ray response fits the data at doses $\geq$ 1 Gy, but significantly underestimates the effect of X rays at lower doses.

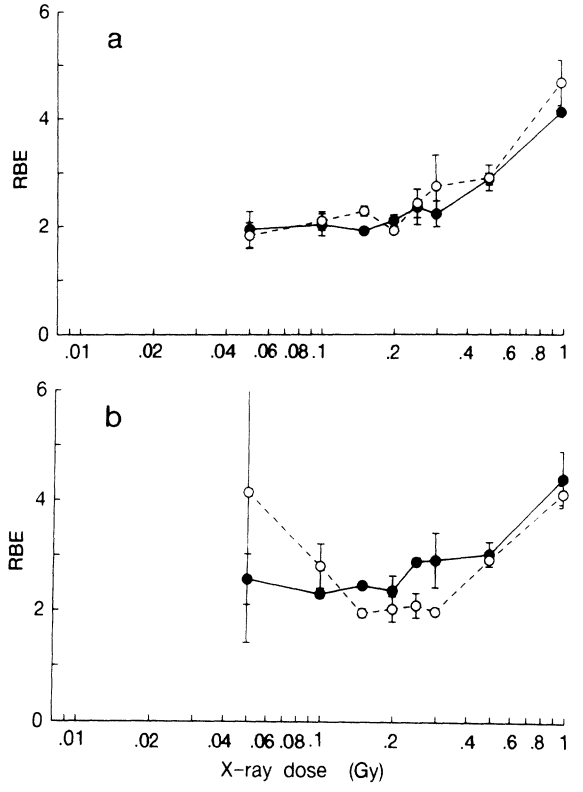

FIG. 5. Two separate experiments (a and b) comparing the surviving fraction of populations of previously unirradiated cells (●) and cell populations irradiated 24 h previously with 1 Gy of 250-kVp X rays (○), after exposure to doses of X rays in the range 0.05–1 Gy. For the pre-irradiated cells, surviving fraction after the subsequent dose of X rays was measured relative to "controls" receiving 1 Gy alone. X-ray dose rate was 0.44 Gy min^{-1}. The data are expressed as RBE by referencing each measurement of X-ray survival to the fit to survival measurements on cells receiving neutrons alone within the same experiment (see text). Each point shows the mean of three measurements ± SEM.

structure in some mammalian survival curves could be a consequence of the differing radiosensitivity of cells in different phases of the cell cycle within an asynchronous population (e.g., *13*). The data in Fig. 7 show that the low-dose X-ray response, summarized by the RBE, is essentially similar for asynchronous cells and populations of cells predominantly in G_1 and S phase, as determined either by elutriation (Fig. 7a) or by individual cell recognition using the DMIPS with phase-specific algorithms (Fig. 7b). Although we have not been able to obtain pure populations of cells in G_1 or S phase with this cell line (see Table I) and have been unsuccessful in obtaining enriched populations of G_2 + M-phase cells, the substantial enrichment to 70–80% in S phase and 80–90% in G_1 phase and the similarity of the low-dose responses despite this suggest that an explanation for the increased low-dose sensitivity based on the cell cycle is unlikely. Interestingly, RBE was independent of cell cycle phase. This was because overall, cells in S phase were more radioresistant to X rays than cells in G_1, as expected, but were also more resistant to neutrons in similar proportion (data not shown).

The same pattern of increasing RBE with increasing X-ray dose was also seen when cells were irradiated at each of the three standard dose rates over the dose range 0.01–1 Gy (Fig. 8a) and with a variable dose rate at each level of dose with a fixed exposure time of 10 s (Figs. 8b and 8c). These data indicate that low-dose X-ray hypersensitivity, as detected in the experiments summarized in Figs. 2, 3, and 4, is unlikely to be a result of changes in dose rate or exposure time associated with the different doses given in these experiments (see Materials and Methods).

DISCUSSION

We have found that cells responded as expected to X-ray doses above 1 Gy with a smooth monotonically downward-bending survival curve, with its zero-dose origin at the value of 1.0 for surviving fraction. Above 1 Gy, the linear-quadratic formulation of the dose–survival relationship described the data adequately. However, for X-ray doses < 1 Gy, we found an increased effect per unit dose of radiation

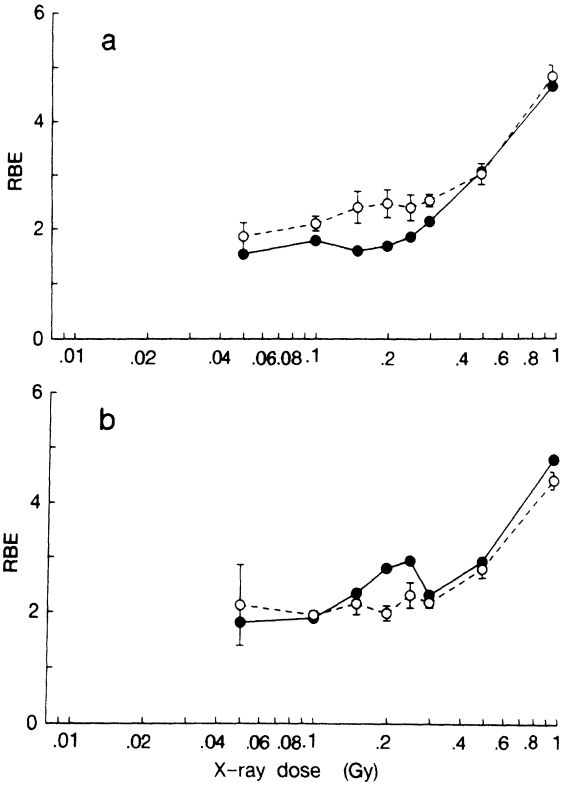

FIG. 6. A comparison of the surviving fraction of cells in the "parental" cell stock (●, one measurement) and cells in two different populations (a and b) cloned from single cells of the parental cell population (○, mean of at least three measurements ± SEM). Data are expressed as RBE (as for Fig. 5).

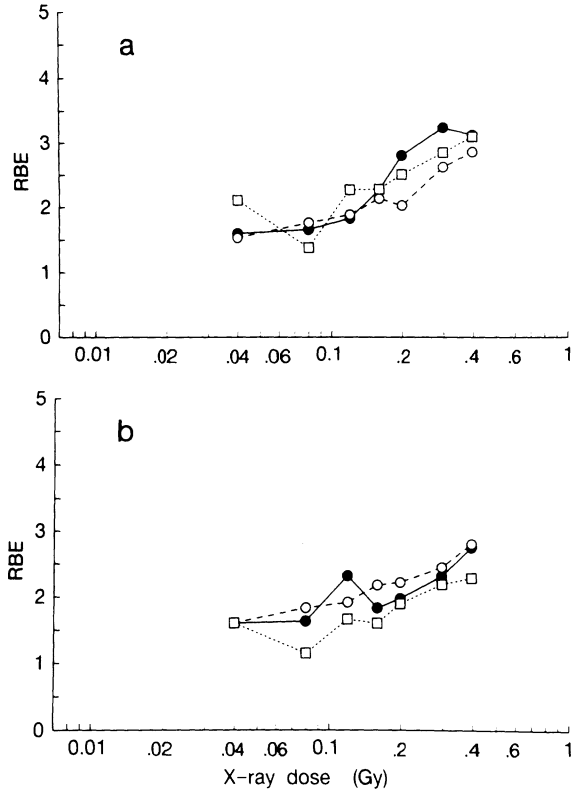

FIG. 7. RBE for asynchronous (●), G_1-phase-enriched (○), and S-phase-enriched (□) cell populations. RBE values were calculated by comparing individual X-ray survival measurements on each phase-specific cell sample with the neutron response of cells in the same phase. (a) Cell populations synchronized by centrifugal elutriation; (b) cell populations identified using the DMIPS cell cycle phase recognition algorithms.

compared with higher doses and values of surviving fraction measured were below the cell survival predicted by extrapolation from the data in the dose range 1–10 Gy to lower doses. A failure to predict the response to low doses (<1 Gy) from the fit of simple models like the LQ equation to doses above 1 Gy has also been reported previously *in vivo*. In a pattern similar to that of the data shown in Figs. 3b and 4, the skin and kidney of the mouse were found to be hypersensitive to multiple small X-ray dose fractions compared with larger doses per fraction (*18, 19*).

It is more difficult to gauge if there is evidence for hypersensitivity to low doses of neutrons, but a comparison of Figs. 3a and 3b gives the overall impression that there is no consistent deviation of the high-LET response from a simple monoexponential reduction in cell survival with dose. We therefore postulated that it might be possible to use the response to neutrons within each experiment as an internal control for possible unidentified "factors" which might contribute to interexperimental variation in absolute radiosensitivity, since these factors would be likely to affect both X-ray and neutron sensitivity in similar proportions. A comparison of the effective D_0 for X rays shown in Fig. 3b with the RBE values shown in Fig. 4 seems to support this argument. The y axes in these two figures have been scaled to give the same dimensions to the change in X-ray radiosensitivity in both diagrams, and visually the overall variation in the data is reduced in the RBE plot. The mean coefficient of variation [standard deviation of regression ÷ median RBE or effective D_0, from the fit of an induced repair model to the data (see later)] is 43% for the data expressed as effective D_0 compared with 35% for the data expressed as RBE, confirming this. Because of the slightly improved quality of the X-ray radiosensitivity data obtained by intraexperimental referencing to neutron radiosensitivity, we therefore carried out further examination of the phenomenon of X-ray hypersensitivity by using the RBE data shown in Fig. 4.

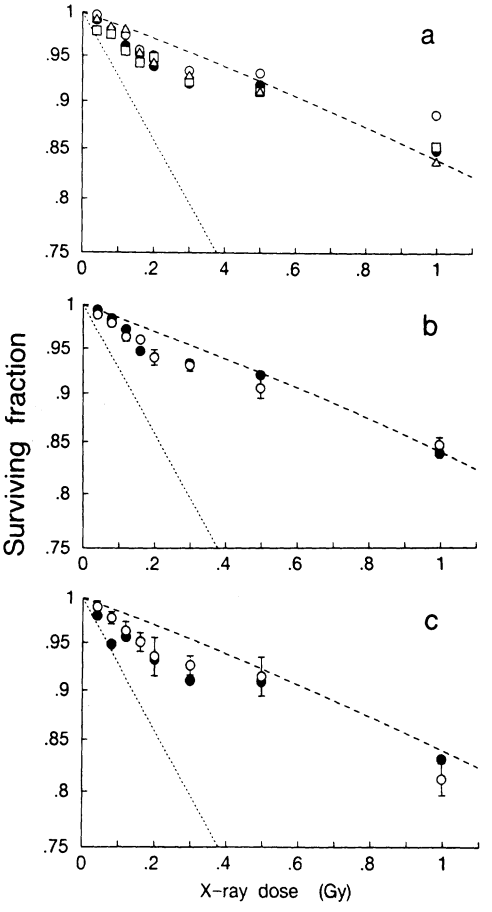

FIG. 8. Survival of cells irradiated with single doses of 250-kVp X rays using one of three dose rates dependent on the dose delivered (see Materials and Methods), as in the experiments summarized in Figs. 3 and 4 (●). (a) 2.5-MVp X rays at each of the three standard dose rates, 0.016 Gy min^{-1} (○), 0.44 Gy min^{-1} (□), and 1.7 Gy min^{-1} (△). (b and c, showing separate experiments) 2.5-MVp X rays with a fixed exposure time of 10 s (○, mean of three samples ± SEM). The dashed line in all graphs is the survival using Eq. (5) with $\alpha = \alpha_{RES}$ and $\alpha/\beta = 9.2$ from Table III. The dotted line shows the fit of a single-exponential function to all 146 measurements of survival of cells irradiated with neutrons.

Possible Biological Variables Not Controlled For

A priori, we could not rule out an influence of changes in dose rate or exposure time on radiosensitivity over the dose range 0–1 Gy. It was expected, however, that since it was the lowest doses that were given at the lowest dose rates, the net X-ray damage per unit dose would, if anything, *decrease* from that with higher doses, in contrast with the effect observed. While it was therefore unlikely that dose-rate effects could account for the shape of the survival curve that we observed, we nevertheless tested the effect of irradiating cells with each of the three standard dose rates over the full dose range 0.01–1 Gy, or a fixed exposure time of 10 s with varying dose rates. Under all these conditions, doses below 0.3 Gy were still more effective per unit dose than higher doses (Fig. 8). At the highest dose of 1 Gy shown in Fig. 8a, there was some evidence that the lower dose-rate exposures were less effective, as would be predicted, but below 0.3 Gy, there was no evidence of a dose-rate effect. Since the dose-rate effect is a consequence of repair, one might tentatively conclude that its absence at these very low doses reflects a lack of repair. This argument is extended later in the discussion.

The experiments summarized in Figs. 5 and 6 suggest that the hypersensitive substructure seen at low doses is not the result of a genetically stable subpopulation of cells with different intrinsic radiosensitivity. However, the majority of the data presented here, notably summarized in Figs. 3 and 4, were obtained using populations of asynchronous cells. This had the advantage that no disruption to the cells occurred during the processes of harvesting from suspension culture, plating, and treatment. However, this also meant that a priori, we could not exclude the possibility that the apparent rapid change in radiosensitivity over the first gray of X-ray dose was due simply to the relative contributions to the overall response from the survival of cells irradiated in different phases of the cell cycle with widely contrasting radiosensitivity. However, the data in Fig. 7 do not support this. Although overall cells in S phase were more radioresistant than cells in G_1, the same substructure was present in the survival response of cells in both phases. Cells in S phase were also more resistant to neutrons, and when X-ray survival was expressed in terms of RBE relative to neutron survival, the data for cells in either phase matched the same pattern of response of asynchronous cells shown in Fig. 4.

However, it was not possible to obtain pure populations with all the cells in any one phase of the cell cycle. Therefore, there still remained the chance that the shape of the survival curve at low doses might be attributable to cells in a particular phase of the cell cycle which formed part of the contaminating fraction in either of the enriched populations (see Table I). To test this hypothesis, the simplest model of cell survival, which assumed the presence of two subpopulations of cells with different X-ray radiosensitivity, was constructed. This model was based on the linear-quadratic dose–survival equation. Assuming a pure exponential response to neutrons,

$$\text{for neutrons, SF} = \exp(-\alpha_N d_N) \quad (1)$$

$$\text{for X rays, SF} = b\exp(-\alpha_s d_X - \beta_s d_X^2) + (1-b)\exp(-\alpha_r d_X - \beta_r d_X^2), \quad (2)$$

where α_s, β_s, α_r, and β_r are the α and β values for the X-ray-sensitive and -resistant subpopulations, respectively, and b is the proportion of sensitive cells in the whole population. In terms of RBE as a function of X-ray dose,

$$RBE = \frac{-\alpha_N d_X}{\log(b\exp(-\alpha_s d_X - \beta_s d_X^2) + (1-b)\exp(-\alpha_r d_X - \beta_r d_X^2))}. \quad (3)$$

This model was well-fitted to both the effective D_0 X-ray data (Fig. 9a) and the RBE data (Fig. 9c) using nonlinear least-squares regression (*20*). However, it predicts that the sensitive subpopulation would consist of about 4% of the cells, and that this small fraction would be about 60 times more radiosensitive than the majority of cells in the population (Table II). This seems unlikely; for example, Sinclair (*21*) reported only an approximate 10-fold variation in the radiosensitivity of mammalian cells *in vitro* between the different phases of the cell cycle.

An Explanation Based on Induced Radioresistance

Inducible protective responses in mammalian cells have been reported in response to a variety of damaging insults (e.g., *22–24*). An inducible repair mechanism was also postulated to explain the multiphasic survival curve in a lepidopteran insect cell line (TN-368) after exposure to X irradiation (*25, 26*). Inducible repair has also been proposed to explain the observations from studies [see (*27*) for summary] in which human lymphocytes irradiated with a small dose of X rays or tritiated thymidine became less susceptible to chromosome aberrations from irradiation given 4–6 h later. In the light of bacterial studies, it is tempting to propose that it might be DNA repair functions that are being induced in these mammalian systems, and this idea now has support from molecular studies showing that specific genes [e.g., *gadd45* (*28*)] and proteins (*29*) can be induced in mammalian cells exposed to X rays. We therefore propose that an X-ray-inducible radioprotective response akin to that demonstrated in human lymphocytes (*27*), V79 cells (*30*), and insect cells (*25, 26*) might also be responsible for the shape of the survival curve reported in this paper. The triggering mechanism for the induction of these radioprotective responses is as yet unknown.

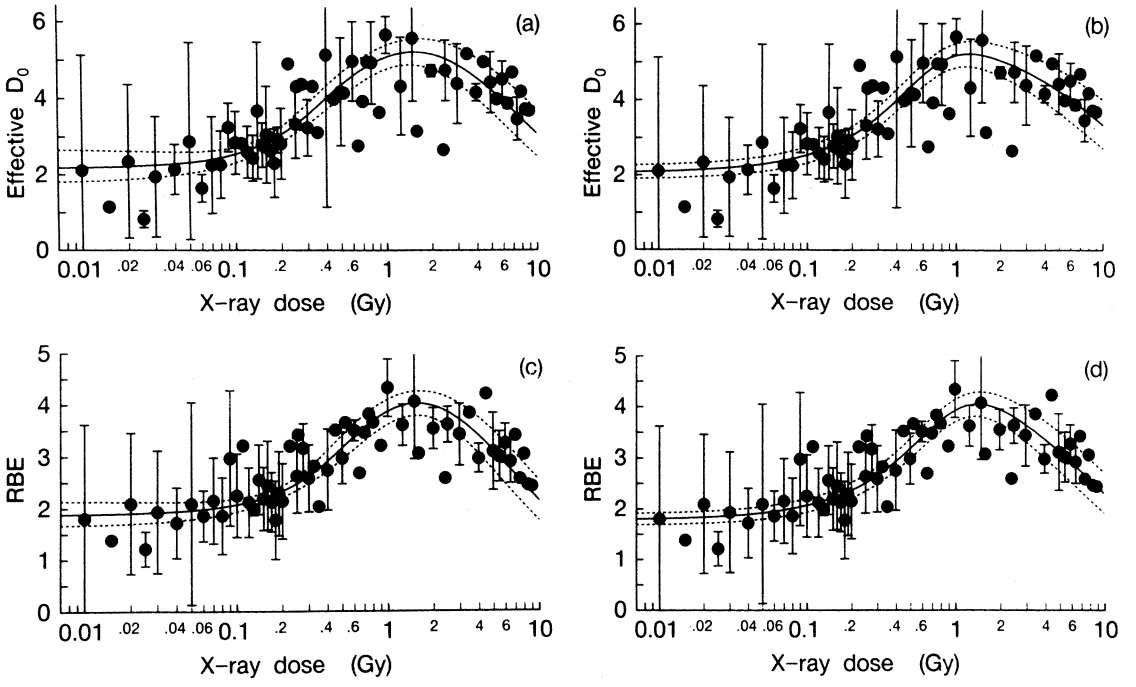

FIG. 9. (a and b) Mean effective $D_0 \pm$ SD; (c and d) mean RBE $\pm$ SD (as in Fig. 4b). The solid lines represent the fit of the two-subpopulation model [a and c, Eq. (2)] or the induced-repair model (b and d, Eqs. (5) and (6)). The dotted lines show the 95% confidence intervals on the mean (expected) predictions from those fits.

Joiner and Johns (*18*) proposed a simple modification to the linear-quadratic representation of the dose–survival relationship in which α decreases with increasing X-ray dose to represent the induced radioresistance. It is important to make α dose-dependent, since the "induction" phenomenon occurs at very low doses where the contribution of βd^2 to the effect is negligible,

$$\text{for neutrons, SF} = \exp(-\alpha_N d_N) \tag{4}$$

$$\text{for X rays, SF} = \exp(-\alpha d_X - \beta d_X^2) \tag{5}$$

and

$$\alpha = \alpha_{RES}(1 + g\exp(-d/d_c)), \tag{6}$$

where d_c represents the dose at which 63% $(1 - e^{-1})$ of induction has occurred and g is the amount by which α at very low doses (α_{SENS}) is larger than α at high doses (α_{RES}). Thus $\alpha_{SENS} = \alpha_{RES}(1 + g)$. Combining Eqs. (4) and (5), the equation for RBE is therefore

$$RBE = \frac{K}{1 + g\exp(-d/d_c) + d_X/V}, \tag{7}$$

where K is α_N/α_{RES} and V is α_{RES}/β (for X rays). This model [Eq. (7)] gives a good fit to the data shown in Fig. 4 (also see Figs. 9b and 9d), using nonlinear least-squares regression (*20*). Table III shows the values of the parameters obtained in these fits. The fits of both the two-population model and the induced repair model to either the effective D_0 or the RBE data are compared in Fig. 9. Although regression statistics were similar for the two fits of the two models, and both models seem to describe the data equally well, the

TABLE II
Values of the Parameters (±SEM; 95% Confidence Limits in Parentheses) in the Two-Subpopulation Model [Eq. (2)] Fitted to Effective D_0 (Fig. 9a) and RBE (Fig. 9c)

Data set	β	α_s	β_s	α_r	β_r
ED_0	0.0414 ± 0.0096 (0.0225–0.0603)	8.07 ± 1.62 (4.88–11.3)	14.4 ± 27.8 (−40.2–69.0)	0.135 ± 0.020 (0.097–0.173)	0.0181 ± 0.0050 (0.0080–0.0281)
RBE	0.0434 ± 0.0123 (0.0193–0.0676)	5.39 ± 1.02 (3.38–7.40)	5.81 ± 9.88 (−13.6–25.2)	0.0914 ± 0.0188 (0.0544–0.128)	0.0180 ± 0.0044 (0.0095–0.0266)

TABLE III

Values of the Parameters (±SEM; 95% Confidence Limits in Parentheses) in the Induced Repair Model (Eq. 6) Fitted to Effective D_0 (Fig. 9b) and RBE (Fig. 9d)

Data set	α_{RES} or K[a]	V	g	d_c
ED_0	0.172 ± 0.014 (0.144–0.200)	13.8 ± 5.8 (2.29–25.2)	1.83 ± 0.24 (1.37–2.30)	0.270 ± 0.049 (0.175–0.366)
RBE	4.86 ± 0.51 (3.86–5.86)	9.16 ± 3.40 (2.49–15.8)	1.73 ± 0.26 (1.22–2.24)	0.382 ± 0.070 (0.244–0.520)

[a] Fit of the model to effective D_0 data gives α_{RES}; fit to RBE data gives K.

induced repair approach has the benefit of simplicity in its mathematical formulation proposed here, having one less parameter.

If induced repair is the explanation of the substructure that we have observed in the survival curve at low doses, then the modified LQ model predicts that radioprotection in V79 cells is triggered over the dose range 0.2–0.5 Gy and that low doses ($\ll$1 Gy) of X rays are 2.2–3.3 times (95% confidence intervals on d_c and $g + 1$; Table III) more effective per unit dose at killing cells than high doses of X rays (>1 Gy), due to *lack* of repair. Interestingly, the value of d_c, the dose required for 63% induction of radioresistance, is similar to values calculated for the normal tissue systems that we have studied [Table III in Ref. (*19*)] although much larger than the doses used to induce radioprotection in lymphocytes (*27*). Even with X-ray doses as high as 0.5 Gy, Goodhead (*31*) has calculated that in each cell only about 20 initial DNA double-strand breaks are produced with maybe 25 times this number of single-strand breaks (SSBs). It therefore seems more likely that "repair induction" is triggered by types of damage (e.g., SSBs) which predominate after low- rather than high-LET irradiation, and this might explain the lack of substructure in the response of cells to low neutron doses (Figs. 2 and 3a). However, highly effective irreparable damage dominates the response to d(4)-Be neutrons to such an extent, producing essentially a linear survival curve, that any substructure due to repair phenomena would be extremely difficult to detect even if it were present. Therefore inducible effects of low doses of high-LET radiation cannot be ruled out, and it would be of interest in the future to study low doses of radiation of intermediate LET, which, although more effective than X rays, still produce downward-bending survival curves in which low-dose substructure might be seen.

Comparison with Other Studies of Mammalian Cell Survival after Low Doses

Low-dose hypersensitivity of mammalian cells to X rays has not been reported in other low-dose studies (*3, 6, 13, 15*), and in fact Skarsgard *et al.* (*13*) found that cells were slightly more *radioresistant* to doses in the range 0.4–2 Gy than predicted by extrapolation from data in the range 4–10 Gy to lower doses, using a linear-quadratic model. Watts *et al.* (*6*) used the same V79 subline and culture procedures as we have used in the present work, with a conventional assay of a large number of cells plated per dose group. However, only X-ray doses down to 0.25 Gy were examined and only 8 individual measurements out of a total of 203 were made at doses less than 0.5 Gy. Figure 4 shows that it would be impossible to verify any increase in effect at low doses unless more substantial work had been done at less than 0.5 Gy and even below 0.25 Gy. In the present study, 278 out of a total of 364 measurements were made at less than 0.5 Gy and 209 measurements were made at less than 0.25 Gy. In the same way, the lowest X-ray dose used in the work of both Skarsgard *et al.* (*13*) and Spadinger and Palcic (*15*) was 0.4 Gy, the only dose group below 0.8 Gy, and it is unlikely that significant hypersensitivity could be detected at this dose level with this small amount of data. The study by Spadinger and Palcic (*15*) is of special interest, however, since they used the same methods of measuring cell survival with a DMIPS cell analyzer as our study presented here.

Skarsgard *et al.* (*13*) and Spadinger and Palcic (*15*) also used V79 hamster cells in their work, but a different subline from that used in the experiments reported here, so it is conceivable that both these studies did not detect low-dose hypersensitivity simply because it was not there in those particular cells, but this seems unlikely. More important may be the use in both studies of a trypsinization procedure for harvesting cells from stock cultures prior to irradiation. If induction of radioresistance with increasing dose is the explanation for low-dose hypersensitivity, then it is possible that even slight damage to cells by agents such as trypsin might trigger the same induction, in which case the effect of subsequent low radiation doses would be less. Our own work presented here did not use trypsin harvesting as our cell stocks were cultured in suspension.

A further hypothesis to explain the discrepancy between our results and the studies by Skarsgard *et al.* (*13*) and Spadinger and Palcic (*15*) focuses on the possible effect of trypsinization (or other biochemical methods of detaching cells from the growth surface) on *cell cycle* progression. Suppose the phenomenon we have observed is due *not* to induced radioresistance but to the short time available for repair between irradiation and division for a small cohort of cells in late G_2 phase. This would be dose-dependent, as would be required to explain the effect, because irradiation would delay cells in G_2 phase, allowing a longer time for repair. Assays which then force a delay in cycle progression, and hence a long repair time, at all radiation doses by use of trypsin would be unlikely to detect the hypersensitivity at low relative to high doses. However, this does appear to be unlikely for the reasons discussed above concerning the re-

sults of fitting a two-population model to our data: this predicts that the radiosensitivity of the small cohort in late G_2 phase would be about 60 times the average sensitivity of the rest of the cell population, and this is too large. One would also expect that the phenomenon would be more pronounced in the experiments using cell populations enriched in the S rather than the G_1 phase; the data in Fig. 7 show that this is not the case.

It is worth raising a further point with reference to the work by Watts *et al.* (*6*) and Skarsgard *et al.* (*13*), which may be regarded as "conventional" assays in the sense that the measure of cell survival is the total number of colonies counted at the end of a growth period. Although the *initial* number of cells seeded is known with greater precision than usual (for different reasons in the two studies), the final number of colonies produced will depend on the ability of cells to attach and grow, and this determines the plating efficiency. However, secondary seeding could occur as cells which round up during division become loosely attached to the growth surface, increasing the chance that a daughter cell might float off and resettle some distance away to form a satellite colony. In conventional assays, this would increase the plating efficiency, but in the DMIPS recognition assay this is less likely as only the *original* positions at which cells were logged are scored to determine colony formation: there would be a low probability that a reseeded cell would settle in the vicinity of a logged position since the total area scanned for colonies at logged positions in a typical experiment composes only 5% of the area scanned initially for the presence of single cells just after treatment. Secondary seeding could explain plating efficiencies greater than 100% which sometimes occur in conventional assays (see Fig. 1, for example), but more importantly this phenomenon could also be dose-dependent. Thus cells irradiated with very low doses which produce little or no delay in cell cycle progression would have less time to attach firmly to the growth surface before the first division than cells in which higher doses produced more substantial delay before division. Therefore, measurements of cell survival may be increased relative to the true value at low but not high doses, leading to the loss of the substructure shown in Fig. 2 (DMIPS assay) in a conventional assay. We are currently using the DMIPS machine in an attempt to test this hypothesis.

Significance for Radiosensitivity Measurements

If induced repair is the correct explanation for the substructure in the cell survival curve which we have seen at low doses, then an implication is that radiosensitivity may be governed largely by the amount of repair, with variations in initial DNA damage and tolerance to residual DNA injury being less important (*32*). This is supported by the hypersensitivity to radiation of cells and tissues with genetic conditions which are characterized by a defect in an aspect of DNA repair, for example, Ataxia telangiectasia, Fanconi's anemia, Cockayne's syndrome (*33*), and xeroderma pigmentosum (*34*). Therefore, one could further hypothesize that variations in radiosensitivity among cell lines, tumors, and other tissues might be due largely to differences in the degree of repair induction in response to radiation. A measurement of surviving fraction at >1 Gy should therefore be an adequate predictor of clinical radiosensitivity, as this is in excess of the dose required to induce repair and clinical radiotherapy uses doses per fraction > 1 Gy. Conversely, any predictions of clinical radiosensitivity made with doses less than 1 Gy might be suspect, as would any comparison between the "true" initial slopes of survival curves which should be much steeper than expected from examination of measurements made above 1 Gy, as illustrated in Fig. 2.

As reducing dose rate and increasing number of fractions are biologically equivalent in radiotherapy, it may therefore be questioned whether predictions of clinical radiosensitivity made from the effect of low dose-rate exposures of 0.01–0.05 Gy min^{-1} (e.g., *35*) are suspect in light of our results. Although we have not yet determined whether increased cell killing per unit dose can be detected as the dose *rate* is reduced, Crompton *et al.* (*36*) have measured enhanced *mutation* at the *hprt* locus in the same V79-379A cell line, after irradiation with protracted single X-ray doses below a very low *dose rate* of only ~0.05 Gy h^{-1}. This implies that dose rates of >0.01 Gy min^{-1} should be "fully inducing" and therefore *should* accurately reflect the response to acute doses of >1 Gy. By using the mathematical relationship between dose rate in a single protracted exposure and number of fractions in biologically equivalent acute exposures developed by Liversage (*37*), 0.05 Gy h^{-1} translates into a notional dose per fraction of 0.2 Gy (assuming a half-time for repair of 1.5 h), very similar to the values of d_c shown in Table III.

CONCLUSIONS

(1) Single X-ray doses in the range 0.01–0.2 Gy are more effective per gray at killing cells than doses > 1 Gy. This results in an X-ray survival curve with substructure at low doses. For neutrons, cell survival reduced exponentially with dose with no evidence of significant substructure.

(2) The low-dose substructure in the X-ray survival curve is unlikely to be due to an artifact of the assay, to the response of cells in a particular phase of the cell cycle, to an effect of the X-ray dose rate or length of the radiation exposure, or to the response of a stable genetic subpopulation of cells.

(3) A plausible explanation of the data is that the low-dose sensitivity reflects the induction of radioprotective mechanisms triggered by increased levels of damage.

ACKNOWLEDGMENTS

This work was supported entirely by the Cancer Research Campaign of the UK. We thank Ms. Helen Johns for assistance in preparing these data for publication.

RECEIVED: March 3, 1992; ACCEPTED: July 15, 1992

REFERENCES

1. T. T. Puck and P. I. Marcus, Action of X rays on mammalian cells. *J. Exp. Med.* **103,** 653–666 (1956).
2. J. W. Boag, The statistical treatment of cell survival data. In *Cell Survival after Low Doses of Radiation: Theoretical and Clinical Implications* (T. Alper, Ed.), pp. 40–53. Wiley, London, 1975.
3. J. S. Bedford and H. G. Griggs, The estimation of survival at low doses and the limits of resolution of the single-cell-plating technique. In *Cell Survival after Low Doses of Radiation: Theoretical and Clinical Implications* (T. Alper, Ed.), pp. 34–39. Wiley, London, 1975.
4. E. J. Hall, Biological problems in the measurement of survival a low doses. In *Cell Survival after Low Doses of Radiation: Theoretical and Clinical Implications* (T. Alper, Ed.), pp. 13–53. Wiley, London, 1975.
5. B. Palcic, J. W. Brosing, G. K. Y. Lam, and L. D. Skarsgard, The requirement of survival measurements at low doses. In *Proceedings, Berkeley Conference in Honor of Jerry Neyman and Jack Kiefer* (L. M. Le Cam and R. A. Olshen, Eds.), pp. 331–342. Wadsworth, New York, 1983.
6. M. E. Watts, R. J. Hodgkiss, N. R. Jones, and J. F. Fowler, Radiosensitisation of Chinese hamster cells by oxygen and misonidazole at low X-ray doses. *Int. J. Radiat. Biol.* **50,** 1009–1021 (1986).
7. T. Alper, *Cell Survival after Low Doses of Radiation: Theoretical and Clinical Applications.* Wiley, London, 1975.
8. B. Palcic, J. W. Brosing, and L. D. Skarsgard, Survival measurements at low doses: Oxygen enhancement ratio. *Br. J. Cancer* **46,** 980–984 (1982).
9. B. Palcic and L. D. Skarsgard, Reduced oxygen enhancement ratio at low doses of ionizing radiation. *Radiat. Res.* **100,** 328–339 (1984).
10. B. Palcic, B. Faddegon, B. Jaggi, and L. D. Skarsgard, Automated low dose assay system for survival measurements of mammalian cells *in vitro. J. Tissue Cult. Methods* **8,** 103–107 (1983).
11. B. Palcic, B. Faddegon, and L. D. Skarsgard, The effect of misonidazole as a hypoxic radiosensitizer at low dose. *Radiat. Res.* **100,** 340–347 (1984).
12. B. Palcic and B. Jaggi, The use of solid state sensor technology to detect and characterise live mammalian cells growing in tissue culture. *Int. J. Radiat. Biol.* **50,** 345–352 (1986).
13. L. D. Skarsgard, I. Harrison, and R. E. Durand, The radiation response of asynchronous cells at low dose: Evidence of substructure. *Radiat. Res.* **127,** 248–256 (1991).
14. L. D. Skarsgard and I. Harrison, Dose dependence of the oxygen enhancement ratio (OER) in radiation inactivation of Chinese hamster V79-171 cells. *Radiat. Res.* **127,** 243–247 (1991).
15. I. Spadinger and B. Palcic, The relative biological effectiveness of 60-Co gamma-rays, 55 kVp X-rays, 250 kVp X-rays, and 11 MeV electrons at low doses. *Int. J. Radiat. Biol.* **61,** 345–353 (1992).
16. I. Spadinger, S. S. S. Poon, and B. Palcic, Automated detection and recognition of live cells in tissue culture using image cytometry. *Cytometry* **10,** 375–381 (1989).
17. I. Spadinger, S. S. S. Poon, and B. Palcic, Effect of focus on cell detection and recognition by the cell analyzer. *Cytometry* **11,** 460–467 (1990).
18. M. C. Joiner and H. Johns, Renal damage in the mouse: The response to very small doses per fraction. *Radiat. Res.* **114,** 385–398 (1988).
19. M. C. Joiner, The dependence of radiation response on the dose per fraction. In *The Scientific Basis for Modern Radiotherapy* (N. J. McNally, Ed.), BIR Report 19, pp. 20–26. British Institute of Radiology, London, 1989.
20. SAS-STAT User's Guide, Version 6, Vol. 2, pp. 1135–1193. SAS Institute, Cary, NC, 1989.
21. W. K. Sinclair, Cell cycle dependence of the lethal radiation response in mammalian cells. *Curr. Top. Radiat. Res. Q.* **7,** 264–285 (1972).
22. L. Samson and J. L. Schwartz, Evidence for an adaptive DNA repair pathway in CHO and human skin fibroblast cell lines. *Nature* **287,** 861–863 (1980).
23. S. Lindquist, The heat shock response. *Annu. Rev. Biochem.* **55,** 1151–1191 (1986).
24. S. S. Gupta and S. B. Bhattacharjee, Induction of repair functions by hydrogen peroxide in Chinese hamster cells. *Int. J. Radiat. Biol.* **53,** 935–942 (1988).
25. T. M. Koval, Multiphasic survival response of a radioresistant lepidopteran insect cell line. *Radiat. Res.* **98,** 642–648 (1984).
26. T. M. Koval, Inducible repair of ionising radiation damage in higher eukaryotic cells. *Mutat. Res.* **173,** 291–293 (1986).
27. S. Wolff, J. K. Wiencke, V. Afzal, J. Youngblom, and F. Cortes, The adaptive response of human lymphocytes to very low doses of ionizing radiation: A case of induced chromosomal repair with the induction of specific proteins. In *Low Dose Radiation: Biological Bases of Risk Assessment* (K. F. Baverstock and J. W. Stather, Eds.), pp. 446–454. Taylor & Francis, London, 1989.
28. M. A. Papathanasiou, N. C. K. Kerr, J. H. Robbins, O. W. McBride, I. Alamo, S. F. Barrett, I. D. Hickson, and A. J. Fornace, Induction by ionizing radiation of the *gadd*45 gene in cultured human cells: lack of mediation by protein kinase C. *Mol. Cell Biol.* **11,** 1009–1016 (1991).
29. D. A. Boothman, I. Bouvard, and E. N. Hughes, Identification and characterization of X-ray-induced proteins in human cells. *Cancer Res.* **49,** 2871–2878 (1989).
30. T. Ikushima, Chromosomal responses to ionizing radiation reminiscent of an adaptive response in cultured Chinese hamster cells. *Mutat. Res.* **180,** 215–221 (1987).
31. D. T. Goodhead, The initial physical damage produced by ionizing radiations. *Int. J. Radiat. Biol.* **56,** 623–634 (1989).
32. S. Powell and T. J. McMillan, DNA damage and repair following treatment with ionizing radiation. *Radiother. Oncol.* **19,** 95–108 (1990).
33. E. C. Friedberg, *DNA Repair.* Freeman, New York, 1985.
34. J. E. Cleaver, Defective repair replication of DNA in xeroderma pigmentosum. *Nature* **218,** 652–656 (1968).
35. G. G. Steel, J. M. Deacon, G. M. Duchesne, A. Horwich, L. R. Kelland, and J. H. Peacock, The dose-rate effect in human tumor cells. *Radiother. Oncol.* **9,** 299–310 (1987).
36. N. E. A. Crompton, B. Barth, and J. Kiefer, Inverse dose-rate effect for the induction of 6-thioguanine-resistant mutants in Chinese hamster V79-S cells by ^{60}Co gamma rays. *Radiat. Res.* **124,** 300–308 (1990).
37. W. E. Liversage, A general formula for equating protracted and acute regimes of radiation. *Br. J. Radiol.* **42,** 432–440 (1969).
38. M. G. Ormerod, A. W. R. Payne, and J. V. Watson, Improved program for the analysis of DNA histograms. *Cytometry* **8,** 637–641 (1987).